International Journal of Electrical, Electronic and Communication Sciences
ISSN: 2517-9438
Vol:9, No:6, 2015

Wind Diesel Hybrid System without Battery Energy Storage Using Imperialist Competitive Algorithm

H. Rezvani, A. Hekmati

***Abstract*—**Nowadays, the use of renewable energy sources has been increasingly great because of the cost increase and public demand for clean energy sources. One of the fastest growing sources is wind energy. In this paper, Wind Diesel Hybrid System (WDHS) comprising a Diesel Generator (DG), a Wind Turbine Generator (WTG), the Consumer Load, a Battery-based Energy Storage System (BESS), and a Dump Load (DL) is used. Voltage is controlled by Diesel Generator; the frequency is controlled by BESS and DL. The BESS elimination is an efficient way to reduce maintenance cost and increase the dynamic response. Simulation results with graphs for the frequency of Power System, active power, and the battery power are presented for load changes. The controlling parameters are optimized by using Imperialist Competitive Algorithm (ICA). The simulation results for the BESS/no BESS cases are compared. Results show that in no BESS case, the frequency control is more optimal than the BESS case by using ICA.

***Keywords*—**Renewable Energy, Wind Diesel System, Induction Generator, Energy Storage, Imperialist Competitive Algorithm.

I. Introduction

A WIND Diesel Hybrid System (WDHS) is a system that produces energy from wind generators and diesel generators (DGs) in order to achieve the maximum electrical power [1]. The main goal of power systems is fuel consumption, operating costs of the system, and environmental impacts. If systems are designed that DGs run full time, WDHS is divided into systems with low to medium penetration. If WDHS is able to bypass DGs, WDHS is classified into High penetration of wind. Penetration of systems is defined based on the penetration of wind energy [2] including:

$$Energy\ Penetration = \frac{Wind\ Turbine\ Annual\ Energy\ Output\ (kWh)}{Annual\ Primary\ Energy\ Demand\ (kWh)} \quad (1)$$

When (1) it is less than 20%, WDHS is defined as having the low penetration rate and when (1) it is between 20% and 50%, WDHS is defined as having the high penetration rate.

Several articles have been proposed to simulate dynamic WDHS and have studied WDHS without energy storage along with some chaos including Wind Turbine Generator (WTG) connection to the DG network. In [3], WDHS with flywheel energy storage variable speed is simulated by hydrostatic transducer. In [4], WDHS with high penetration rate of wind including a DG and a clutch is studied. In [5], Battery-based Energy Storage System (BESS) is studied generally. In [6], BESS has been investigated to increase power output of a wind farm. This paper aims to WDHS simulation and improve dynamic system.

H. Rezvani is with Department of Electronics, Islamic Azad University Central Tehran Branch, Iran (corresponding Rezvani to provide phone: +989126016193; fax: 021-66760784; e-mail: haniyehrezvani@gmail.com).
A. Hekmati is with Department of Electronics, Shahid Beheshti University, Iran (e-mail: a_hekmati@sbu.ac.ir).

II. WDHS Structure

Fig. 1 consists of a DG, a WTG, and two operational modes, that is, diesel-only (DO) and wind-diesel (WD). In DG mode, DO is active, and reactive power is needed to supply the loads. In this case, WTG is off, and therefore Ct=0. Also, the governor is responsible for speed, DE control, and adjustments of the frequency and voltage settings. In WD case, WTG provides active power. In this case, regulators are responsible to control voltage and frequency, the same as the case of DO (Ct=ON) [7].

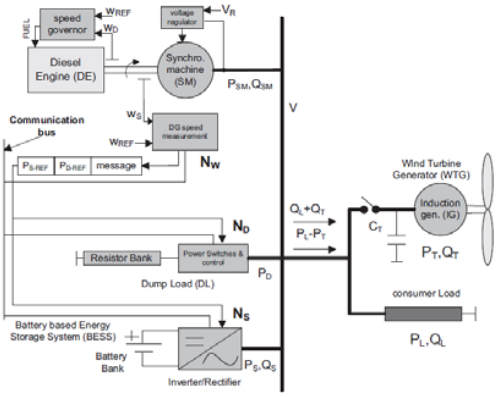

Fig. 1 WDHS [7]

As shown in Fig. 1, WTG stimulates an induction generator (IG) connected directly to an independent network.

The mechanical power is:

$$P_{T-M} = \frac{1}{2}\rho A v^3 C_p \quad (2)$$

where ρ is the air density, v is the wind speed, A is the area swept by the turbine blades and C_P is the power coefficient of blades. C_P is a function of the Tip Speed Ratio:

$$TSR = \frac{Rw_r}{v} \quad (3)$$

where R is blade length and w_r is shaft speed.

The pitch control is not used here, and C_P is a function of TSR. In addition, changes in the speed range of IG are very

limited. Consequently, C_P is assumed as a function of wind speed. As wind speed is semi-random, there is no method to control WTG's active power. Therefore, WTG is considered as an uncontrollable source of active power.

In WD, WTG produces P_T power which is higher than consumption-power of P_L charge. So, active output power of powerhouse, $P_L - P_T$, is negative. It means that DG power should be negative to make active consumption and productive powers to equal levels in order to fix the frequency. Dump load (DL) should be inserted in the system to avoid inversion of DG [8]. In order to keep a positive DG productivity, WDHS commands the DL to consume the required amount of power. In this case, DG could control the frequency. In Fig. 1, DL includes some switches and a resistance bank. DL consumption of active power is controlled by opening and closing of these switches. Consequently, they can be used as a control source of active power [8].

Energy saving system (ESS) [9] is used to avoid inversion of the DG in WD mode. In Fig. 1, BESS includes a capacitor bank and a power converter. It converts DC/AC for different levels of battery. In addition, BESS can save or detect the required energy. Therefore, it is used as active power control source.

III. The Control System

A distributed control system (DCS) is applied in the power system to control DL and BESS. A DCS [10] includes several CPUs and are connected together by a communication network. As shown in Fig. 1, the DCS consists of three nodes including a sensor node for the measurement of speed of DG shaft N_W and two driving shafts of N_D and N_S. Sensor node of N_W includes a Proportional-Integral (PI). Its input is frequency error e_f ($e_f = f - f_N$), where f_N is the power system-rated frequency and f is the current frequency. Its output is the reference power P_{REF}. So, K_P and K_I are proportional and integral gains, respectively.

$$P_{REF} = K_P e_f + K_I \int e_f dt \quad (4)$$

The Integral part of PI increases speed and stability response of the system. The PI proportion part makes BESS and DL increase the system load when frequency is higher than the rated value (e_f>0). In addition, BESS produces power when frequency is less than the rated value (e_f <0). This is a kind of speed control which improves system transition. N_W usually calculates the distributed power between BESS and DL when P_{REF} >0. The reference power to be dump by DL and the reference power to be stored/ retrieved By BESS, Therefore:

$$P_{REF} = P_{S-REF} - P_{D-REF} \quad (5)$$

$$P_{D-REF} = 0 \text{ if } P_{REF} < P_{S-N} \quad (6)$$

In order to maintain synchrony between DL and BESS actuators when P_{REF} >0, the sensor node N_W should communicate with $P_{S\text{-}REF}$ and $P_{D\text{-}REF}$ to actuator nodes N_D and N_S by network. This message is periodic and ensures that both drivers can receive reference at the same time.

IV. Imperialist Competitive Algorithm

Fig. 2 shows the flowchart of the Imperialist Competitive Algorithm (ICA). This algorithm starts by generating a set of candidate random solutions in the search space of the optimization problem. The generated random points are called the initial countries. Countries in this algorithm are the counterpart of chromosomes in GAs and Particles in Particle Swarm Optimization (PSO), and it is an array of values of a candidate solution of optimization problem. This array is given by [10]:

$$country = |y_1, y_2, y_3, \dots, yN_{var}| \quad (7)$$

where y_i's are the variables and N_{var} is the dimension of the optimization problem.

The cost function of the optimization problem determines the power generation of each country. Based on their power, some of the best initial countries (the countries with the least cost function value), become imperialists and start taking control of other countries (called colonies) and form the initial empires [11]. The cost is obtained by:

$$cost = f(country) = f(y_1, y_2, y_3, \dots, yN_{var}) \quad (8)$$

Two main operators of this algorithm are assimilation and revolution. Assimilation makes the colonies of each empire get closer to the imperialist state in the space of sociopolitical characteristics (optimization search space). Revolution brings about sudden random changes in the position of some of the countries in the search space. During assimilation and revolution, a colony might reach a better position and has the chance to take the control of the entire empire and replace the current imperialist state of the empire [11].

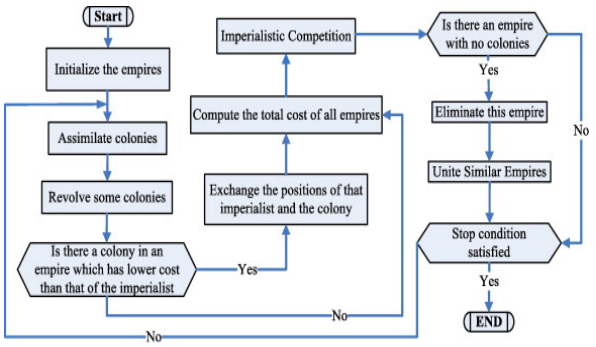

Fig. 2 ICA flowchart

Imperialistic Competition is another part of this algorithm. All the empires try to win this game and take possession of colonies of other empires. In each step of the algorithm, based on their power, all the empires have a chance to take control of one or more of the colonies of the weakest empire [12].

Algorithm continues with the mentioned steps (assimilation, revolution, competition) until a stop condition is satisfied.

This algorithm has a high accuracy and high speed; the cost function used in this step includes integral of input error of controllers. The programmed optimization platform has been prepared by using MATLAB. The parameters of the ICA which are used for this model are in Table I.

TABLE I
ICA PARAMETERS

Parameter	Value
Number Of Countries	50
Number Of Imperialist	6
Maximum Iteration	20

ICA is used to determine the optimum coefficients of controllers. According to the ICA, K_I and K_P values are as follows:

TABLE II
VALUE OF K_I AND K_P

Parameter	K_I	K_P
Diesel Generator	1.4691	10^{-3}
Dump Load	39.1700	200
Bess	646.1442	0.5

V. SIMULATION SCHEMATICS

Fig. 3 shows the simulation structure of WDHS by MATLAB. There are some descriptions about some parts such as the IG and the SM, loads, and three-phase breaker in detail.

SM has a nominal power of 300 kVA. It receives the DE mechanical power output of DE block.

WTG's constant speed stall control [12] includes an IG connected directly to network and wind turbine block. WT block includes WT power curves, which define mechanical power in WT shaft as a function of wind speed and speed of WT shaft. WT mechanical power is determined by the speed of WT shaft to be able to calculate the arrival charge to the IG power.

Loads include a main load of 150 kW and a load of 100 kW (both resistive). The 150 kW load represents a medium load of WDHS and a 250 kW load represents the maximum load of WDHS. So, when three-phase switch (3PB) changes from open form to close form, the system load increases to maximum amount suddenly. Medium/maximum loads are used in this paper and are close to the 2/3 of daily load pattern of WDHS [13].

DL consists of eight 3-phase resistance [14] connected with GTO switches in series. Resistance values follow 8-bit binary progression; therefore, the consumption power supplies rated voltage of network by DL. Includes:

$$(S_0 + S_1 2^1 + .. + S_7 2^7) P_{STEP} = X_{D-REF} P_{STEP} \quad (9)$$

Equation (9) means that power can change from 0 to 255, directly.

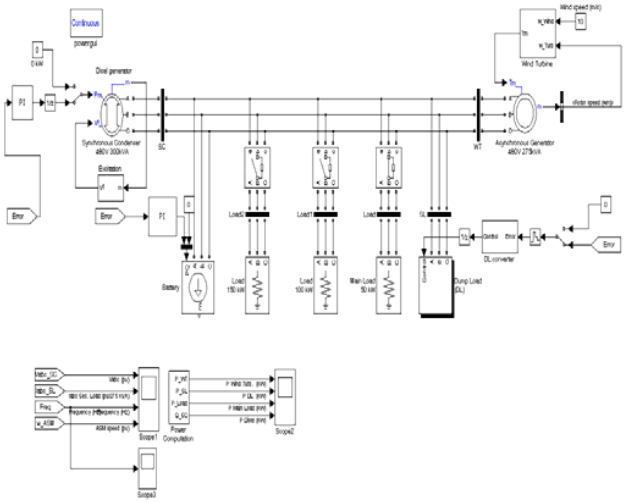

Fig. 3 Matlab-Simulink Model

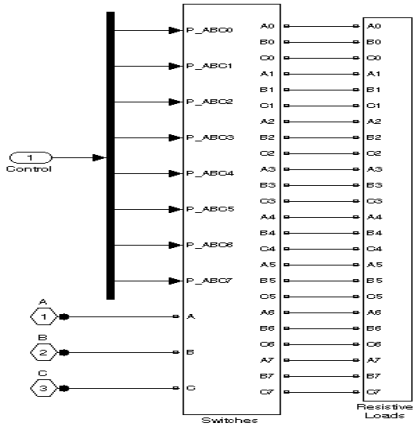

Fig. 4 Block Diagram of Dump Load

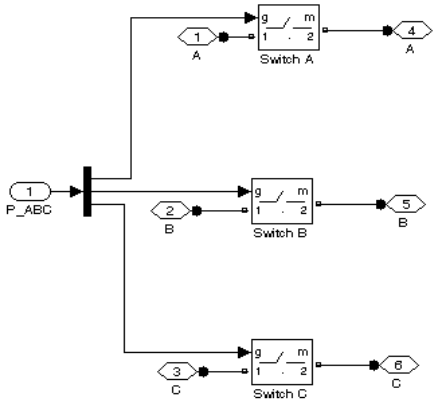

Fig. 5 Block Diagram of GTO switches for one resistor

Voltage level of the battery is determined by the three-phase converter when the battery works in the DC link. Voltage of DC line should be selected more than 10–15% of voltage of inherent DC link in order to calculate oscillations of network, reactive voltage drop of line, and reliability coefficient of performance [15]. DC line voltage is equal to

the peak of line-to-line voltage. Therefore, DC link voltage level, V_{DC}, is defined as:

$$V_{DC} = 1.10 \div 1.15\sqrt{2}V_{LL} \quad (10)$$

V_{LL} is the line-to-line RMS voltage. If the DC voltage is less than the intrinsic DC line voltage, the diode bridges charge the battery and semiconductor switches discharge them. This causes the flow of reactive power between the network and transducer. Having a unit power factor and removing the resistive losses, converter output voltage range should correspond with (11) to assess the validity level of the selected DC line voltage, where:

$$m\frac{V_{DC}}{2} > \sqrt{\frac{2}{3}{V_{LL}}^2 + (wLi_d)^2} \quad (11)$$

m is Modulation index, w is grid pulsation, L is Inductance of coil binding, i_d is direct current of components. The left side of (10) reflects the fact that PWM converter works in the linear region as an ideal voltage source. Modulation index (m) can be used for sinusoidal modulation and for modulation of the state vector. As state vector modulation has better utilization of DC link, and its digital implementation is easier and has fewer ripple current [16]. Therefore, it is used more in simulation.

In addition, the controlling parameters of DL and DG are determined by Cost function. Fig. 6 shows the cost function by MATLAB.

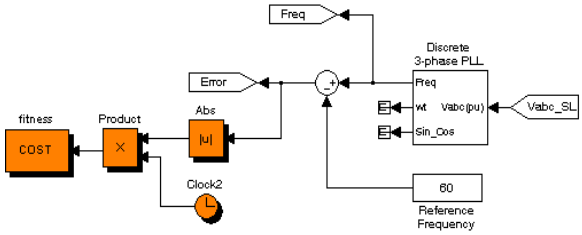

Fig. 6 Block Diagram of Cost function

VI. Simulation Result

In this part, response of WDHS for a consumer load of 100 kW and wind speed of 10 m/s is studied. Such sudden wind change does not occur in a real system. WDHS responses are shown by graphs. Variables of the used graphs include the following:

Frequency system in pu (fpu), active generation of power by the DG and consumption of power by the load (both uncontrollable), manufacture of active power by DG and production/consumption of active power by BESS (both controllable). Power is considered positive for WTG, DG, and BESS if power is produced. Active power is considered positive for load if power is consumed. Figs. 10, 12 and 13 imply on evolutionary process of variables when BESS is on. Figs. 11 and 14 imply on evolutionary process of variables when BESS is off.

Fig. 3 shows the simulation by MATLAB including a DG of 300 kVA capacity and 480 V power, a wind powerhouse with 300 kVA capacity and 480 V power, three main loads, and an adjustable load. Each load enters into the system with intervals.

Fig. 7 shows that in t = 5 s, resistive load of 100 kW is connected by closed 3PB as shown in Fig. 3; it is observed in active power curve of load which shows swinging of the load. Pure resistive load causes the swings.

In t = 10 s, third resistance load of 50 kW is added to network. As shown in Fig. 4, wind power plant cannot supply total power of load since t = 10 s. Consequently, DG should connect with network to supply some power.

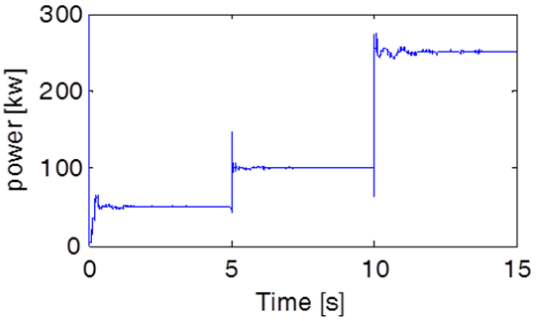

Fig. 7 Load Power

As shown in Figs. 8 and 9, control of frequency when energy storage is eliminated is similar to a case that energy storage is not in the system. Whereas dynamic response and behavior of wind power plant is improved when energy storage is eliminated in the system. Therefore, energy storage is not suitable due to losses and the efficiency of the system.

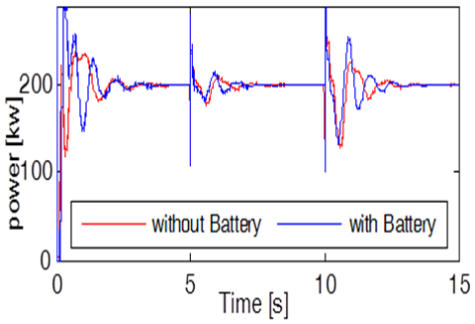

Fig. 8 Wind power for both BESS/ no BESS

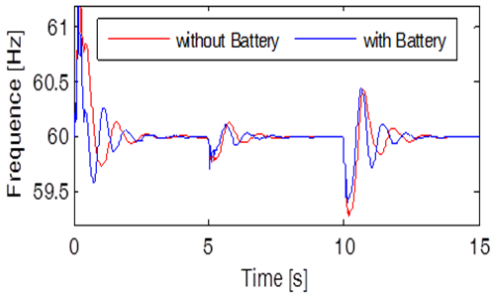

Fig. 9 System Frequency for both BESS/ no BESS

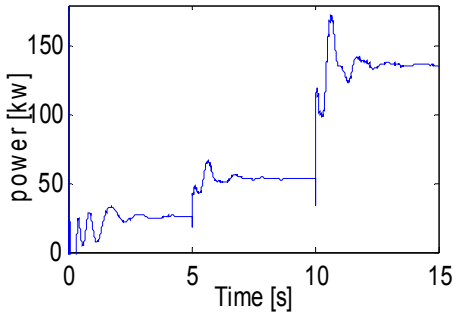

Fig. 10 Diesel Generator Power with BESS

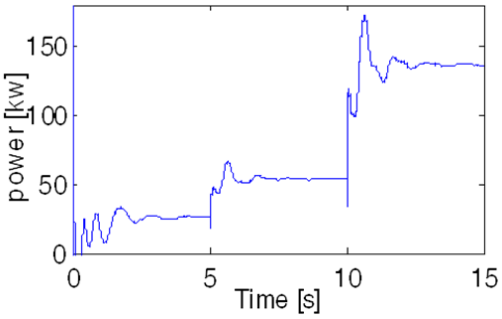

Fig. 11 Diesel Generator Power without BESS

In Fig. 12, by adding loads to system, some changes are created in the battery to control system frequency. In BESS case due to losses, the system frequency is reduced.

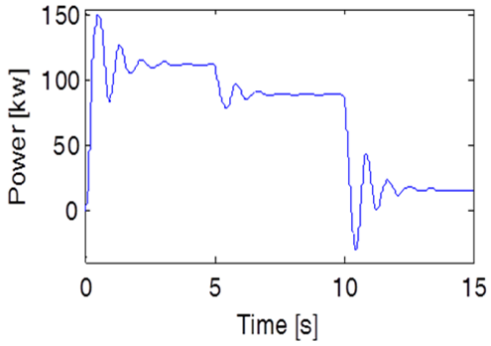

Fig. 12 BESS Power

Figs. 13 and 14 show the power of DL with and without energy storage. This load is used for frequency regulation of system. Speed of response of DL to changes in output power of loads is fast. This response is the same both with and without energy storage.

VII. Conclusion

WDHS component was presented with and without BESS case. In order to obtain the required voltage for battery, a detailed schematic of the Matlab-Simulink model with the calculations was explained. Compared to a non-BESS, applying BESS is not suggested because of the expensive costs, battery loss, and a reduction in the efficiency of the system. Also, it is concluded that the frequency control of system with optimal parameters—when omitting BESS—would stabilize faster.

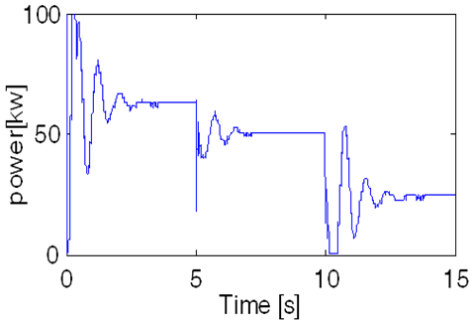

Fig. 13 Dump Load with BESS

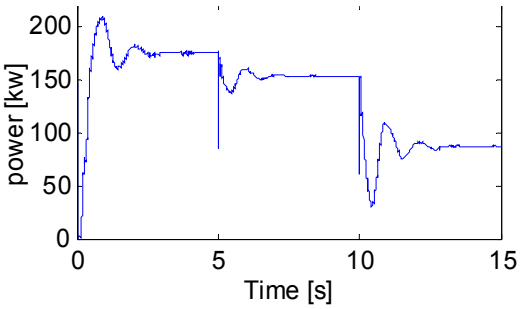

Fig. 14 Dump Load without BESS

Appendix

TABLE III
Induction Generator Data

Parameter	Value
The Nominal Apparent Power	275kVA
The Nominal Line-To-Line Voltage (V_{rms})	480V
The Nominal Frequency (f_{ref})	60HZ
The Stator Resistance (r_s)	0.016pu
The Stator Inductance (L_s)	0.06pu
The Rotor Resistance (r_r)	0.015pu
The Rotor Inductance (L_r)	0.06pu
The Number Of Pole Pairs	2
The Inertia Constant (H)	2s
The Friction Factor (B)	0

TABLE IV
Wind Turbine Data

Parameter	Value
The Nominal Mechanical Power	275kW
The Base Wind Speed	10 m /s

TABLE V
Diesel Generator Data

Parameter	Value
The Nominal Apparent Power	300kVA
The Line-To-Line Voltage	480V

REFERENCES

[1] Wind/Diesel Systems Architecture Guidebook, American Wind Energy Association, 1991.
[2] S. Drouilhet, "High penetration AC bus wind–diesel hybrid power systems", Village Power' 98 Technical Workshop, Washington DC, Octuber 1998.
[3] C. Carrillo, A. Feijóo, J. Cidrás, "Comparative study of flywheel systems in an isolated wind plant", Renewable Energy, vol. 34, pp.890-898, June 2008.
[4] R. Sebastián, R. Pe˜na Alzola, "Effective active power control of a high penetration wind diesel system with a Ni–Cd battery energy storage", Renewable Energy, vol. 35, pp. 952–965 May 2010.
[5] K.C. Divya, Jacob Østergaard, "Battery energy storage technology for power systems– an overview", Electric Power System Research, vol. 79, pp. 511-520, April 2009.
[6] S.M. Muyeen, R. Takahashi, T. Murata, J. Tamura, H. Ali Mohd, "Application of STATCOM/BESS for wind power smoothening and hydrogen generation", Electric Power System Research, vol. 79, pp. 365-373, February 2009.
[7] R. Sebastian, R. Pena Alzola, "Simulation of an isolaed Wind Diesel System with battery energy storage", Electric Power System Research, vol. 81, pp. 677-686, February 2011.
[8] Syed Q. Ali, Hany M. Hasanien, "Frequency Control of Isolated Network with Wind and Diesel Generators by Using Adaptive Artificial Neural Network Controller", International Review of Automatic Control (I.RE.A.CO.), vol. 5, no. 2 ISSN 1974-6059, March 2012.
[9] R. Hunter, D. Infield, S. Kessler, J. De Bonte, T. Toftevaag, B. Sherwin, M. Lodge, G. Eliot, " Wind–Diesel Systems: A Guide to the Technology and Its Implementations", Cambridge University Press, UK, October 2005.
[10] W. Lawrenz, CAN System Engineering: From Theory to Practical Application, Springer London, 2013.
[11] M. Maadi, M. Maadi, "Optimization of Cluster Heads Selection by Imperialist Competitive Algorithm in Wireless Sensor Networks", International Journal of Computer Applications (0975 – 8887), vol. 89, no.19, March 2014.
[12] S. N. Shirkouhi, H. Eivazy, R. Ghodsi, K. Rezaie and E. A. Gargari, "Solving the Integrated Product Mix-Outsourcing Problem by a Novel Meta-Heuristic Algorithm: Imperialist Competitive Algorithm", Expert Systems with Applications, vol. 37, pp. 7615-7626, December 2010.
[13] H.G. Beyer, T. Degner, H. Gabler, "Operational behavior of wind–diesel systems incorporating short-term storage: an analysis via simulation calculations", Solar Energy, vol. 54, pp. 429-439, June 1995.
[14] R. Gagnon, B. Saulnier, G. Sybille, P. Giroux, "Modelling of a Generic High Penetration No-storage Wind–Diesel System Using Matlab/Power System" Blockset, in: Global Windpower Conference, Paris, France, April 2002.
[15] M. Liserre, F. Blaabjerg, A. Dell'Aquila, "Step-by-step design procedure for a gridconnected three-phase PWM voltage source converter", International Journal of Electrons, vol. 91, pp. 445–460, August 2004.
[16] B. Wu, Y. Lang, N. Zargari, S. Kouro, Power Conversion and Control of Wind Energy System, Published in Canada, 2011.